

# Dynamic Oxygen-Enhanced T1-weighted MR in Mouse Tumour Xenografts. Comparison Between Oxygen-Enhanced MRI and DCE-MRI.

I. V. Linnik<sup>1,2</sup>, N. Woodhouse<sup>3</sup>, M. Scott<sup>3</sup>, C. Liess<sup>3</sup>, J. J. Tessier<sup>3</sup>, H. Barjat<sup>3</sup>, G. J. Parker<sup>1,2</sup>, J. C. Waterton<sup>2,3</sup>, and J. H. Naish<sup>1,2</sup>

<sup>1</sup>Imaging Science and Biomedical Engineering, School of Cancer and Imaging Sciences, University of Manchester, Manchester, United Kingdom, <sup>2</sup>Biomedical Imaging Institute, University of Manchester, Manchester, United Kingdom, <sup>3</sup>Imaging, Translational Sciences, AstraZeneca, Alderley Park, Macclesfield, Cheshire, United Kingdom

**BACKGROUND:** Tumour hypoxia plays a pivotal role in malignant progression, metastasis and resistance to various therapies. Recent studies have suggested that oxygen-enhanced (OE) MRI can potentially be used for assessing regional changes of oxygen delivery and accumulation in tumours when switching from breathing air to 100% oxygen, based on T<sub>1</sub>-shortening due to dissolved paramagnetic molecular oxygen.<sup>1, 2</sup> However while many tumours do show the expected R<sub>1</sub> increase, we have previously observed large regions counter-intuitively exhibiting apparent R<sub>1</sub> reduction.

**PURPOSE:** To characterise the R<sub>1</sub>-increasing and R<sub>1</sub>-decreasing domains in OE-MRI in terms of their DCE-MRI response.

**METHODS:** MICE: The experiments were carried out in compliance with the UK Animals (Scientific Procedures) Act. Male nude mice (n=6) with human glioblastoma xenografts (U87-MG) implanted on their right flank were anaesthetised throughout imaging with 1.5 – 1.9% isoflurane in either air, or 100% oxygen. Temperature and respiration rate were monitored using SA Instruments equipment (Stony Brook, NY).

MRI: Data were acquired at 9.4T (Varian Inova, USA) with a 38 mm I.D. quadrature volume coil. R<sub>1</sub> was measured prior to both OE-MRI and DCE-MRI using a slice selective IR FLASH sequence<sup>3</sup>: TR/TE= 21 ms/2.2 ms; flip angle = 20°; 1 average, acq. matrix 128 x 64; inversion slice thickness = 20 mm; FOV = 40mm x 40 mm; 4 axial slices, slice thickness 2 mm; inversion times (TI) of 0.01, 0.25, 0.5, 0.75, 1, 2, 5, 7, 9, and 12 s. OE-MRI and DCE-MRI dynamic data were acquired using a T<sub>1</sub>-weighted 2D FLASH sequence with the same parameters as the IR FLASH sequence, but with no inversion preparation. OE-MRI dynamic sequence was run continuously over 10 min: 2 min breathing air, 6 min - 100% O<sub>2</sub>, then 2 min - air. DCE-MRI data were acquired over 8 min, 2 min baseline acquisition and 6 min post gadopentetate tail vein injection (0.3 mmol/kg).

ANALYSIS: A region of interest encompassing the whole tumour was delineated on each slice. Baseline R<sub>1</sub> on air, R<sub>1</sub> on oxygen and ΔR<sub>1</sub> (oxygen minus air) were measured for each voxel in the tumour. t-statistic maps of ΔR<sub>1</sub> air-oxygen calculated from each voxel's time series allowed identification of sub-regions of R<sub>1</sub>-increasing/R<sub>1</sub>-decreasing voxels (p ≤ 0.05). For DCE-MRI, the signal intensity was measured for each voxel in the tumour over time then converted to a change in 1/T<sub>1</sub> (R<sub>1</sub>) as a measure of Gd-DTPA concentration. Area under the curve whilst breathing 100% oxygen (AUC-O<sub>2</sub>) and initial area under the concentration curve up to 120s post-Gd-DTPA injection (IAUC<sub>120</sub>) were derived.

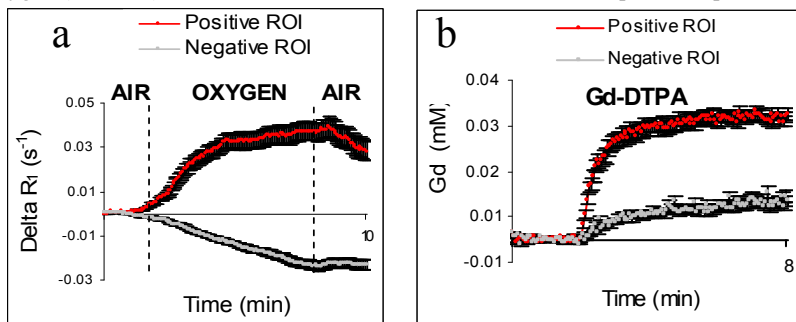


Fig.1. Dynamic OE (a) and GD-DTPA (b) uptake curves for R<sub>1</sub>-increasing (mean value – red, SD – black) and R<sub>1</sub>-decreasing parcellations (mean value – grey, SD – black) under 100% oxygen inhalation.

**RESULTS:** Fig.1a shows the R<sub>1</sub> change over dynamic acquisition for R<sub>1</sub>-increasing and R<sub>1</sub>-decreasing parcellations under 100% oxygen inhalation averaged over all tumours. The Gd-DTPA concentration time curves for the same regions are shown in Fig. 1b. DCE-MRI data exhibit high contrast uptake in the R<sub>1</sub>-increasing parcellations and very low Gd-DTPA uptake in the R<sub>1</sub>-decreasing parcellations.

**DISCUSSION:** Some domains exhibited an immediate significant increase in R<sub>1</sub> following the switch to oxygen inhalation, consistent with the previously reported.<sup>1, 4</sup> These correspond to high Gd uptake and represent well-perfused/oxygenated tumor regions. The domains that showed apparent R<sub>1</sub> reduction following the switch to oxygen inhalation corresponded to low DCE enhancement. Oxygen-induced vascular steal, fluctuating perfusion, R<sub>2</sub>\* and R<sub>2</sub> changes, and haemoglobin oxygenation resulting in decreased concentration of paramagnetic deoxyhaemoglobin,<sup>5, 6</sup> might all in principle induce apparent R<sub>1</sub> reduction. Changes in blood volume and blood flow can counteract the effect of blood oxygenation, and changes in blood pH and glucose levels can alter oxygen extraction. Despite these potential confounds, the complexity of the interpretation in absence of histology correlation and the fact that tissue oxygenation is both affected by oxygen supply (via perfusion) and oxygen utilisation, the correspondence between the oxygenated tumor regions as measured by OE-MRI and the regions associated with increased blood perfusion as measured by DCE-MRI provide a strong indication that the OE-MRI results correspond to a genuine physiological response to the oxygen challenge.

**CONCLUSIONS:** Tumour regions, which increase R<sub>1</sub> with the switch to oxygen, are well-perfused while tumour regions, which reduce R<sub>1</sub> with the switch to oxygen, are poorly-perfused.

**REFERENCES:** 1: O'Connor *et al*, *Int J Radiat Oncol Biol Phys*, 1-7, 2009. 2: Matsumoto *et al*, *Magn Reson Med*, 56: 240-246, 2006. 3: Haase *et al*, *Magn Reson Med*, 13: 77-89, 1990. 4: Linnik *et al*, *Proc. Intl. Soc. Mag. Reson. Med.* 17, 4367, 2009. 5: Meyer *et al*, *Magn Reson Med.*, 34: 234-41, 1995. 6: Blockley *et al*, *Magn Reson Med.*, 60: 1313-1320, 2008.

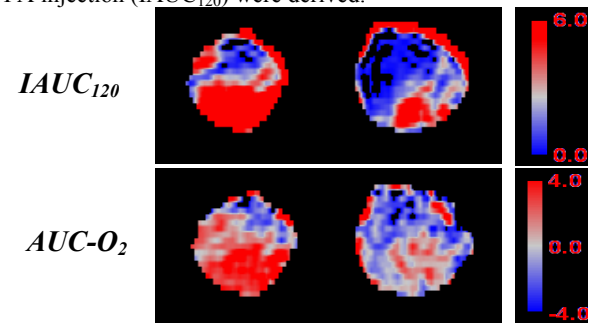


Fig.2 Example Gd-based IAUC<sub>120</sub> and AUC-O<sub>2</sub> maps in 2 slices from a representative tumour.